BHM (2011) Vol. 156(11): 450 – 456
DOI 10.1007/ s00501-011-0035-y
Printed in Austria

BHM Berg- und Hüttenmännische Monatshefte

Sub-Critical Crack Growth in Alumina – a Comparison of Different Measurement and Evaluation Methods

Tanja Lube[1] and Robert G. A. Baierl[2]

[1] Institut für Struktur- und Funktionskeramik, Montanuniversität Leoben, Franz-Josef-Straße 18, 8700 Leoben, Austria
[2] Linde Material Handling GmbH, Großostheimer Straße 198, 63741 Aschaffenburg, Germany

Received July 8, 2011; accepted October 17, 2011

Keywords: sub-critical crack growth, alumina, constant stress-rate tests, static bend tests

Schlagworte: unterkritisches Risswachstum, Aluminiumoxid, konstante Spannungsrate, statische Biegeversuche

Sub-Critical Crack Growth in Alumina – a Comparison of Different Measurement and Evaluation Methods

Tanja Lube[1] Robert G. A. Baierl[2]

[1] Institut für Struktur- und Funktionskeramik, Montanuniversität Leoben, Franz-Josef-Straße 18, 8700 Leoben, Austria
[2] Linde Material Handling GmbH, Großostheimer Straße 198, 63741 Aschaffenburg, Germany

Abstract: Every brittle failure of a ceramic component is preceded by a certain amount of sub-critical crack growth (SCCG). In order to incorporate lifetime predictions into design considerations, material data on this phenomenon have to be known. Such material data are only available for a few materials. This is primarily due to the fact that the necessary experiments are time consuming and the evaluation of the data may be complicated.

In this work two common measurement methods, static bend tests and constant stress-rate tests were used to determine the parameters for sub-critical crack growth, *n* and *B* of a commercial alumina ceramic. Several evaluation procedures were applied to the constant stress-rate data. The data evaluation turned out to be straightforward because a clear separation of the inert strength plateau from the SCCG influenced strength could be observed. A large range of stress-rates spanning five orders of magnitude could be used for the evaluation.

All evaluation procedures lead to comparable values for *n* and *B*, constant stress-rate tests provide more accurate values for the SCCG parameters than the evaluation of the lifetime distribution. While *n* could be determined with reasonable scatter, the variety in *B* was much bigger.

Unterkritisches Risswachstum in Aluminiumoxid – Ein Vergleich verschiedener Mess – und Auswertemethoden

Zusammenfassung: Jedem spröden Bruch eines Keramikbauteiles geht ein gewisses Maß an unterkritischem Risswachstum voraus. Um diesem Phänomen bei der Auslegung von Bauteilen durch Lebensdauervorhersagen Rechnung tragen zu können, müssen die entsprechenden Materialkennwerte bekannt sein. Solche Daten stehen bisher nur für wenige Keramiken zur Verfügung. Das liegt unter anderem daran, dass die nötigen Experimente zeitaufwändig sind, und die Auswertung mitunter durch die Datenstreuung verkompliziert wird.

In dieser Arbeit wurden zwei bekannt Messmethoden – statische Biegeversuche und Biegeversuch mit konstanter Lastrate – verwendet, um die Parameter des unterkritischen Risswachstums, *n* und *B*, eines kommerziell erhältlichen Aluminiumoxids zu messen. Dabei wurden die Biegeversuch mit konstanter Lastrate mit verschiedenen Methoden ausgewertet. Es stellte sich heraus, dass die Auswertung im untersuchten Fall einfach durchzuführen war, da es eine klare Trennung des Bereichs der Inertfestigkeit von jenem gab, wo die Festigkeit lastratenabhängig ist. Zur Auswertung konnte ein Lastratenbereich von fünf Größenordnungen herangezogen werden.

Alle Messmethoden und Auswertungen resultierten in vergleichbaren Ergebnissen für *n* und *B*. Die Daten, die aus der Lebensdauerverteilung gewonnen wurden, zeigen allerdings eine größere Streuung.

1. Introduction

When we observe the strength of ceramic materials, some facts that clearly discern their behaviour from the one known for metals appear: the strength shows (i) a considerable variability, (ii) a volume dependence and (iii) it is also time dependent – even at room and low temperatures. The first two items can be explained by the brittle nature of ceramics and the fact that they always contain crack-like defects due to processing or machining. According to basic fracture mechanics relations[1], failure occurs when the stress intensity $K_{I,appl}$ at the most dangerous defect a due to the stress σ

$$K_{I,appl} = \sigma Y \sqrt{\pi a}\,, \tag{1}$$

is equal to or exceeds the fracture toughness K_{Ic}. Y is a geometry factor that is tabulated in textbooks for selected loading cases[2]. Strength is thus inversely proportional to the square root of the size of the critical defect. The statistical distribution of defect sizes leads thus to a considerable variation of strength values measured on a set of nominally identical specimens. This scatter is usually described using the Weibull distribution[3],

$$F(\sigma) = 1 - \exp\left[-\frac{V}{V_0}\left(\frac{\sigma}{\sigma_0}\right)^m \right] \quad , \tag{2}$$

which gives the probability of failure F of a specimen/component with volume V at the stress σ. The distribution function is characterised by the Weibull parameter m and the characteristic strength σ_0, V_0 is a normalising volume.

Since the probability of finding a big defect (that causes a low strength) is higher in a larger volume of material under stress, the strength of this larger volume is also expected to be lower as compared to the strength of a smaller volume.

It has additionally been observed that the strength of ceramics also depends on time. Failure occurs after some time under a (low) load which causes a $K_{I,appl}$ below the critical stress intensity K_{Ic}, or that the strength decreases as the loading rate is decreased. This reduction in strength, which is caused by the growth of the pre-existing defects, is called sub-critical crack growth (SCCG), because during the time dependent process[4] $K_{I,appl} < K_{Ic}$. The dominant mechanism for SCCG at low and intermediate temperatures is a breaking of the chemical bonds at the crack tip due to a stress-assisted reaction with any polar species present in the environment[5]. The typical response of ceramic materials to SCGG is shown in Fig. 1 where the crack growth velocity v is plotted as a function of $K_{I,appl}$. For engineering purposes region I with typical crack growth rates between 10^{-13} m s^{-1} to 10^{-6} m s^{-1} is most important[4,6,7]. Here, the material behaviour can be described by a Paris type law

$$\mathrm{v} = \frac{\mathrm{d}a}{\mathrm{d}t} = \mathrm{v}_0 \left(\frac{K_I}{K_{Ic}}\right)^n \tag{3}$$

where v_0 and the exponent n are (temperature dependent) material parameters. The exponent n is in the range of $n = 20$ to $n = 200$[4,6,7]. As analyses show, SCCG has a significant influence on the strength and lifetime in a wide range of loading conditions[6,8]. It can be assumed that SCCG precedes every brittle failure to a certain extend. Therefore there is a need to characterise ceramic materials with respect to their SCCG properties. Such material data do exist only for a few materials because the necessary experiments are time consuming and the evaluation of the data may – in certain cases - not be straightforward[9,10].

Several methods for the experimental determination of the SCCG behaviour of ceramics have been proposed[11], some of which will be introduced in the following section. They differ in experimental effort, in the range of crack growth velocities that govern failure and in the necessary prior knowledge of other material properties[6,12]. The scope of the present investigation is to compare some of these methods.

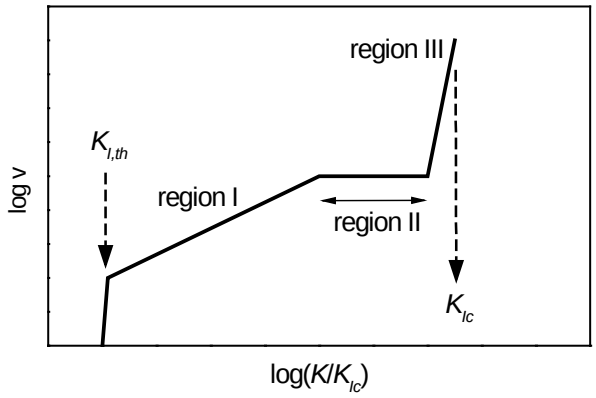

Figure 1: Schematic of a typical v-*K*-curve for ceramics.

2. Experimental Methods to Determine SCCG Parameters

The description of the experimental methods for the determination of the SCCG parameters in this section is intentionally presented in a condensed form, because more detailed derivations can easily be found in textbooks[6,13]. Generally the lifetime t_f of a specimen can be determined for any stress history $\sigma(t)$ by integration of eq. (3) considering that v = da/dt and thus dt = 1/v da and by using eq. (1).

$$\int_0^{t_f} \sigma(t)^n \mathrm{d}t = \frac{1}{\mathrm{v}_0} \int_{a_i}^{a_c} \left(\frac{K_{Ic}}{Y\sqrt{\pi a}} \right)^n \mathrm{d}a \quad . \tag{4}$$

During SCCG, cracks grow from their starting size a_i to the final (= critical) size a_c. Strictly speaking, the geometry factor Y depends on the crack length but for small cracks this dependence is weak and can be neglected. The integration of eq. (4) then leads to

$$\int_0^{t_f} \sigma(t)^n \mathrm{d}t = B \cdot \sigma_i^{n-2} \cdot \left[1 - \left(\frac{a_i}{a_c} \right)^{(n-2)/2} \right] = B \cdot \sigma_i^{n-2} \cdot \left[1 - \left(\frac{\sigma_b}{\sigma_i} \right)^{(n-2)/2} \right] \quad . \tag{5}$$

with

$$a_c = [K_{Ic} / (\sigma_b Y \sqrt{\pi})]^2 \tag{6}$$

for the strength σ_b of a specimen containing a defect of size a_c and

$$a_i = [K_{Ic} / (\sigma_i Y \sqrt{\pi})]^2 \quad , \tag{7}$$

which correlates the starting defect size a_i with the "inert strength" σ_i, i.e. the strength without any SCCG and the abbreviation

$$B = \frac{2K_{Ic}^2}{(n-2)\,\mathrm{v}_0\,\pi Y^2} \quad . \tag{8}$$

2.1. Static Bend Tests

In static bending tests a constant stress σ_{stat} is applied to the specimen and the time to failure is measured. For this loading case, eq. (5) can be further evaluated to

$$t_f = B\,\sigma_i^{n-2}\,\sigma_{stat}^{-n} \quad , \tag{9}$$

because $(a_i/a_c)^{(n-2)/2} \approx 1$. A number of static bend tests performed at different stress levels σ_{stat} allows the determination of the parameters n and $B\,\sigma_i^{n-2}$ from a linear regression of the data plotted as log σ_{stat} versus log t_f.

2.2. Scatter of Lifetime

The inert strength and the lifetime in static bend tests at σ_{stat} are both determined by the initial defect size. The scatter of inert strength values and the scatter of lifetimes, $F(t_f)$, can be described by the Weibull distribution $F(\sigma_i)$, eq. (2). To obtain the function $F(t_f)$, σ_i in $F(\sigma_i)$ has to be replaced by a rearranged form of eq. (9). This results in

$$F\left(t_f\right) = 1 - \exp\left[-\left(\frac{t_f}{t_0} \right)^{m^*} \right] \quad , \tag{10}$$

with

$$m^* = \frac{m}{n-2} \qquad . \tag{11}$$
$$t_0 = B\, \sigma_0^{n-2}\, \sigma_{stat}^{-n}$$

The parameters of the lifetime distribution, m^* and t_0, can be obtained in a similar way as the parameters of the strength Weibull distribution by using the maximum likelihood method[6,14]. For a further calculation of n and B through eq. (11), the knowledge of the parameter of the inert strength distribution, m and σ_0 is mandatory.

2.3. Constant Stress-Rate Tests ("dynamic" bend tests)

In constant stress-rate tests – the standardised method to determine the SCCG parameters[15] – bend specimens are tested with various loading rates $\dot{\sigma}$ until failure. The relation between loading rate and strength σ_b can be derived by using the time differential expressed as $\mathrm{d}t = \mathrm{d}\sigma / \dot{\sigma}$ in eq. (5). The integration then leads to the implicit relation

$$\sigma_b^{n+1} = (n+1)\, \dot{\sigma}\, B\, \sigma_i^{n-2} \left[1 - \left(\frac{\sigma_b}{\sigma_i} \right)^{n-2} \right] \quad . \tag{12}$$

For high loading rates, $\dot{\sigma} \to \infty$, eq. (12) approaches $\sigma_b = \sigma_i$, while for low loading rates, $\dot{\sigma} \to 0$ it can be simplified to

$$\sigma_b^{n+1} = B\,(n+1)\, \sigma_i^{n-2}\ \dot{\sigma} \quad . \tag{13}$$

Experiments for the determination of the SCCG parameters are usually performed at several low loading rates and eq. (13) is used for the evaluation of the data. The parameter n can be obtained from the slope $1/(n+1)$ of a linear regression of the data in a plot log σ_b versus log $\dot{\sigma}$ and the quantity $B\, \sigma_i^{n-2}$ from the intercept. A further calculation of the material parameters v_0 according to eq. (8) requires the knowledge of K_{Ic} and Y. For the purpose of lifetime prediction[11] or the construction of "strength – probability – time" (SPT)-diagrams[17] it is however sufficient to know B.

3. Investigated Material and Experimental Details

Experiments were performed on standard bend bar specimens ($3 \times 4 \times 45$ mm^3) of a commercial 99.7% Al_2O_3 (Frialit-Degussit F99,7 by Friatec AG, D-68229 Mannheim, BRD) in 4-point flexure[16]. The nominal support span was 40 mm and the loading span was 20 mm for all tests. All experiments were conducted at room temperature (~ 21 °C) in laboratory air (~ 30% rel. humidity). Strength tests and constant stress-rate tests were conducted on a Schenk Hydropuls system with various loading rates and pre-loads. Static bend tests were performed on custom made test rigs with dead weight loading at a single mean static stress level of σ_{stat} = 270 MPa. The stress level was chosen to achieve failure in less than 168 h (two weeks). The inert strength distribution and the lifetime distribution were determined on samples containing N = 30 specimens each. A loading rate of 1000 MPa s^{-1} was used for the inert strength measurements. The parameters of the

Weibull distributions of the inert strength and the lifetime were evaluated by the maximum likelihood procedure described in EN 843-5[14]. Biased values for m and m^* are reported. Constant stress-rate tests were conducted at stress-rates of 0.000833 MPa s^{-1}, 0.01 MPa s^{-1}, 0.1 MPa s^{-1}, 1 MPa s^{-1}, 100 MPa s^{-1} and 10^5 MPa s^{-1}. Seven specimens were tested at each stress-rate. Pre-loads of 240 MPa and 250 MPa, respectively, were applied at 1 MPa s^{-1} to keep the test duration reasonably short for the tests at 0.000833 MPa s^{-1} and 0.01 MPa s^{-1}.

The material has a density of $\rho = 3.93\ 10^3$ kg m^{-3}, and a Youngs modulus of $E = 380$ GPa[18]. Fracture toughness was determined to be $K_{Ic} = 3.7 \pm 0.2$ MPa $m^{0.5}$ on five specimens using the SEVNB-method[19].

4. Results

The measured strength and lifetime data are plotted in "Weibull"-diagrams, i.e. a linear representation of eq. (2) or eq. (10), respectively, in Fig. 2. The results of the statistical evaluation are presented in Tab. 1, the resulting SCCG parameters n and B can be found in Tab. 2.

Table 1: Parameters of the Weibull distributions for the inert strength and the lifetime at 270 MPa. Numbers in brackets refer to the 90% confidence intervals.

inert strength		**lifetime**	
$\sigma_0 = 395.2$ MPa	[387.6 – 403.1]	$t_0 = 40750$ s	[22281 – 75026]
$m = 17$	[12.8 – 20.9]	$m^* = 0.554$	[0.41 – 0.67]

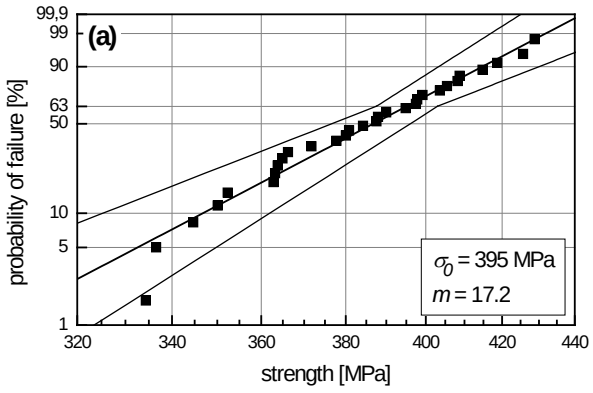

Figure 2a

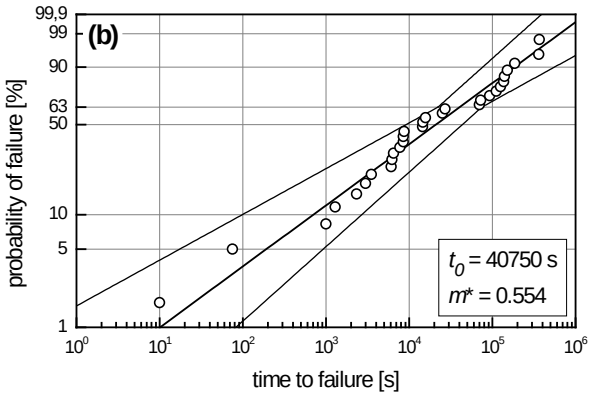

Figure 2b

Figure 2: Weibull distributions of (a) the inert strength and (b) the lifetime at $\sigma_{stat} = 270$ MPa. The borders of the 90% confidence intervals are indicated.

Table 2: Results of the fits of eq. (13) to constant stress-rate data using different methods. Numbers in brackets refer to the 90% confidence intervals.

method	**slope**	**intercept**
all data	0.02907 [0.0261 – 0.0325]#	336.83 [331.53 – 341.24]#
mean at each $\dot{\sigma}$	0.02904	336.77
median at each $\dot{\sigma}$	0.03104	338.83
σ_0 at each $\dot{\sigma}$	0.02975	344.86

#Bootstrap analysis

The results of the constant stress-rate tests are plotted as $\log\sigma$ versus $\log\dot{\sigma}$, according to eq. (13) in Fig. 3. Both asymptotic regions predicted by the theoretical derivation are clearly distinguishable: at stress-rates $\dot{\sigma} > 100\ \mathrm{MPa\,s^{-1}}$ the data fall into the inert strength regime, while a decrease of strength with decreasing stress-rate is observed at rates $\dot{\sigma} \le 100\ \mathrm{MPa\,s^{-1}}$. These data were evaluated by fitting with eq. (13)[20]. The line shown in Figure 3 is a plot of eq. (12) using the results from this evaluation. The data were also evaluated using the mean values[15], the median and the Weibull characteristic strength values at each stress-rate. The results of these fitting procedures are summarised in Tab. 2, the evaluated crack growth parameters *n* and *B* are in Tab. 3. To get an estimate of the 90% confidence bands of the result for *n*, two different procedures were used. A Bootstrap analysis was performed for the evaluation of all data points with $\dot{\sigma} \le 100\ \mathrm{MPa\,s^{-1}}$. Bootstrap confidence intervals are obtained by randomly choosing *k* samples with replacement from the original data (here $k = 1000$). The fitting is performed on all of these samples and thus a distribution function of the fit parameters can be obtained. The confidence intervals for the *n* found with the other evaluation procedures were calculated using the data given by Peterlik[21].

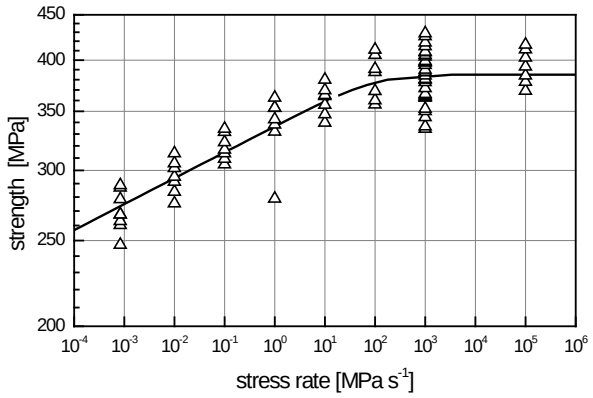

Figure 3: Plot of the strength values measured at various constant stress-rates. The data used to determine the inert strength distribution are included. The line indicates a plot of eq. (12) using the *n* and *B* determined by using all data with $\dot{\sigma} \le 100\ \mathrm{MPa\,s^{-1}}$.

Table 3: Comparison of results for the SCCG parameters *n* and *B* obtained by different testing and evaluation methods. Numbers in brackets refer to the 90% confidence intervals.

method	***n* [-]**		***B* [(MPa)^2 s]**
lifetime distribution	32.7	[28 – 44]	22181 [12128 – 40840]
constant stress-rate tests – all data	33.2	[29.6 – 36.3]$^{\#}$	16705 [14997 – 18256]$^{\#}$
constant stress-rate tests – mean	33.4	[27.2 – 39.6]*	16048
constant stress-rate tests – median	31.2	[25.3 – 37.1]*	23800
constant stress-rate tests – σ_0	32.6	[27.8 – 37.4]*	18835

$^{\#}$Bootstrap analysis
*according to data given in[9]

5. Discussion

The results presented in Tab. 3 show that all methods lead virtually to the same value for the crack growth exponent *n*. The confidence interval for the results from the lifetime distribution is much bigger than those for all other evaluations. As shown in literature[9,21,22] all evaluation methods for the constant stress-rate data give the correct expectation value for *n*, but the fit on the Weibull characteristic strength values leads to the lowest standard deviation. The differences are however very small. The confidence interval for the evaluation of all data is smaller than those of all other methods. This can be due to the fact that the data given by Peterlik[21] which were used for the

calculation of the intervals refer to slightly different experimental conditions. They were generated for five stress-rates and 10 tests at each rate, while here we have used six stress-rates with seven tests.

From the data in Tab. 3, it appears that all methods lead to different results for the quantity *B*. Recognizing the overlapping confidence intervals it can, however, be concluded that they cannot be distinguished on the basis of the number of tests that were performed.

5.1. Evaluation of Constant Stress-Rate Tests

The evaluation of constant stress-rate tests is complicated by several issues. An obvious one is the use of a pre-load for the tests at the two lowest stress-rates. The pre-load was applied fast to avoid SCCG during this test step. In principle, the use of a pre-load leads to a reduced amount of SCCG during the constant stress-rate test (as compared to a zero pre-load). Therefore, the strength with a pre-load is higher than the strength without a pre-load. The effect of the pre-load on the failure stress can be evaluated as follows. Using eq. (5), $(a_i/a_c)^{(n-2)/2} \approx 1$ and $\mathrm{d}t = 1/\dot{\sigma}\,\mathrm{d}\sigma$, it follows for tests without and with pre-load σ_V applied at $\dot{\sigma}_V$

$$B\sigma_i^{n-2} \approx \int_o^{\sigma_b} \frac{\sigma^n}{\dot{\sigma}}\mathrm{d}\sigma \tag{14}$$

$$B\sigma_i^{n-2} \approx \int_0^{\sigma_V} \frac{\sigma^n}{\dot{\sigma}}\mathrm{d}\sigma + \int_{\sigma_V}^{\sigma_{bV}} \frac{\sigma^n}{\dot{\sigma}}\mathrm{d}\sigma \tag{15}$$

with the strength without pre-load, σ_b, and the strength with applied pre-load, σ_{bV}. Equating eqs. (14) and (15) leads to

$$\frac{\sigma_{bV}}{\sigma_b} = \left[1 - \left(\frac{\sigma_V}{\sigma_{bV}}\right)^{n+1}\left(1 - \frac{\dot{\sigma}}{\dot{\sigma}_V}\right)\right]^{-\frac{1}{n+1}} . \tag{16}$$

For $\dot{\sigma}/\dot{\sigma}_V << 1$ this simplifies to

$$\frac{\Delta\sigma}{\sigma_B} = \left[1 - \left(\frac{\sigma_V}{\sigma_{bV}}\right)^{n+1}\right]^{-\frac{1}{n+1}} - 1 \quad . \tag{17}$$

A plot of this relation for different ratios σ_V/σ_{bV} is shown in Fig. 4. The error in the failure stress due to a pre-load is so small that it is masked by other measurement uncertainties or the statistical variation of strength. The effect of the pre-load on failure strength can therefore be neglected.

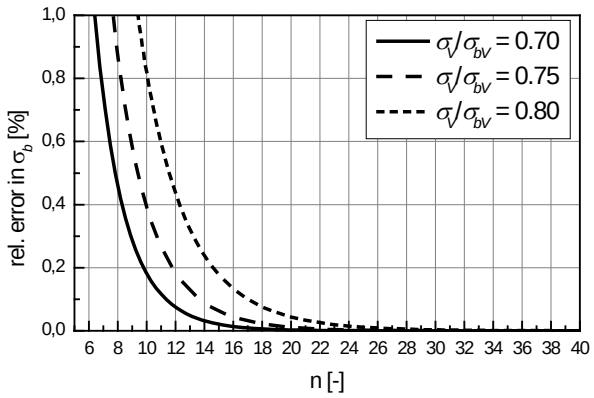

Figure 4: Influence of a pre-load on the failure stress for different ratios σ_V/σ_{bV} under the assumption that the ratio that the stress-rate during the strength test is a least ten times faster than the pre-load application rate.

Other issues are caused by the statistical nature of the strength of ceramics. On the one hand not only the inert strength of ceramics is distributed, but also – with different distribution parameters that are directly related to those of the inert strength distribution - the strength at a certain stress-rate. From this it follows that, the lower the inert Weibull modulus *m* is, the higher is the error margin for *n*. On the other hand, high true *n* values lead to a smaller slope $1/(n+1)$ in the diagram and thus a larger error in *n*. The experimental *n* depends on the true *n* and on the Weibull modulus *m*. The higher *m* and the lower *n*, the smaller is the error in the experimental *n*. Apparently, combinations exist which do not allow a determination of *n* using the simple method presented here with an error smaller that 20%[21]. Extremely sophisticated statistical procedures are necessary to evaluate data with unfortunate combinations of *m* and *n*[9,10].

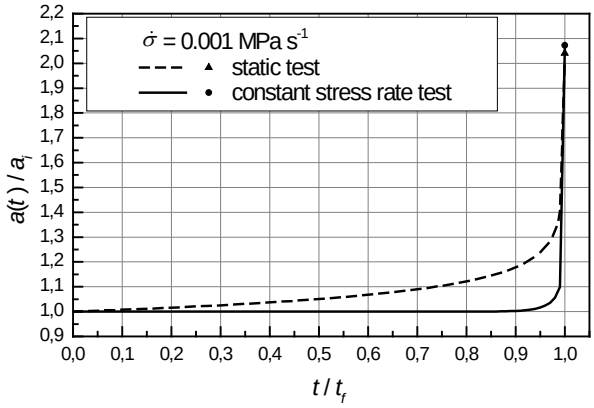

Figure 5: Normalised crack length as functions of normalised test time during static and constant stress-rates test. The symbols indicate the crack length at failure.

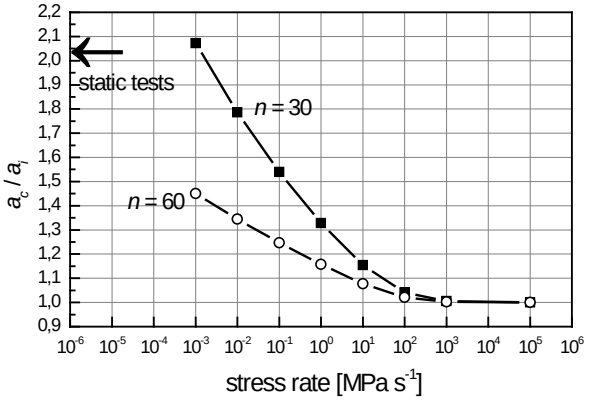

Figure 6: Calculated ratio of crack length at failure, a_c over initial crack length a_i for different test conditions and *n* values.

5.2. Crack Length during Static and Constant Stress-Rate Tests

To investigate the differences in static bend tests and constant stress-rate tests, it is useful to plot the crack length as a function of time, $a(t)$ for both types of tests. $a(t)$ can be obtained by integration of eq. (4) for the two different test conditions. The crack length in static bend tests, $a_{stat}(t)$, and constant stress-rate tests, $a_{csr}(t)$, as functions of time are plotted in Fig. 5. The material properties used for this plot are σ_i = 395 MPa, K_{Ic} = 3.7 MPa m$^{0.5}$, Y = 1.12, n = 30, $v_0 = 10^{-5}$ m s^{-1}, $\sigma_{stat} = 0.7 \cdot \sigma_i$ and $\dot\sigma = 0.001\,\mathrm{MPa\,s^{-1}}$. In both tests the initial crack length is similar, the $t_{f,stat}$ = 7056 s, $a_{c,stat} = 2.04\ a_i$ and $t_{f,csr}$ = 274417 s, $a_{c,csr} = 2.07\ a_i$. In static tests the crack grows from the beginning of the test with an increasing crack growth velocity. The crack spends most of its lifetime in the low velocity range, i.e. in region I of the v-*K*-curve. In constant stress-rate test the crack starts growing after approx. 75% of the test duration. The crack growth velocity increases strongly over more than five orders of magnitude. It should be mentioned, that this normalized plot looks identical for all stress-rates. What changes are the absolute values for the critical crack lengths $a_{c,csr}$ and the times to failure $t_{f,csr}$. This is illustrated in Fig. 6 where a_c/a_i is plotted versus the stress-rate. The ordinate of this diagram can easily be converted to read σ_b/σ_i using eqs. (6) and (7). In the present investigation (with $n \cong 30$) the constant stress-rate tests at slow rates < 100 MPa s^{-1} lead to crack lengths that are substantially longer than the initial crack length, i.e. a significant reduction in fracture stress as compared to the inert strength can be observed (even if the scatter of these data is considered). At the lowest stress-rate the crack length at failure is nearly the same as the one obtained in the static test. For a hypothetical material with just a different n = 60 the increase in

crack length is not so prominent, and the decrease of time dependent strength may be hidden in the scatter of the data. While the lowest five stress-rates were available for the fitting of eq. (13) in the real experiments, only four stress-rates could be used for the hypothetical material with the higher *n*. The scatter in initial crack lengths (related to the Weibull distribution of strength with *m* and σ_0) that leads to a scatter in the critical crack lengths (according to a strength distribution with a different Weibull modulus $m'(m,\dot{\sigma})$) has not yet been taken into account. This inherent scatter leads to scatter bars at each datum in Fig. 6. The higher the Weibull modulus of the material, the smaller are the scatter bars. It is easy to envisage that constant stress-rate tests for materials with a low Weibull modulus and a high *n* cannot be evaluated with sufficient accuracy.

5.3. Comparison of the Experimental Effort

Since both methods presented here lead to nearly the same results, it is worth to compare the experimental effort. The amount of specimens necessary for the lifetime and the inert strength Weibull distribution (60 specimens) is comparable to the number needed for the tests at the seven different constant stress-rates (49 specimens).

A Weibull strength distribution comprising 30 specimens can be measured in approximately two hours. The total experimental time under static stress including specimen handling is approximately 550 h. Since three test rigs were available, this can be reduced to approximately 200 h. No interaction with a running test is necessary, so it is reasonable to estimate an effective experimental time effort of approximately two to four weeks for the static bending tests.

The constant stress-rate test requires a quite dissimilar experimental time. The tests with the four fastest stress-rates (28 specimens) can be performed in the same time as the strength distribution, i.e. 2 h. The tests with stress-rates of 0.01 MPa s^{-1} and 0.1 MPa s^{-1} take between 0.7 h to 1.5 h if a pre-load is used for the slower tests, so that for a total of 14 such tests, 2.5 working days have to be planned. The tests at 0.001 MPa s^{-1} take up to 13 h even if a pre-load is used. In total the effort for the constant stress-rate tests is approximately two weeks.From this point of view both test strategies seem to be equal. It has to be considered though that static tests can only be planned to a certain duration (by choosing the stress level) if the inert strength distribution and a guess value for *n* is known. For the present investigation the static stress level was chosen to produce fracture within two weeks maximum. If *n* is unknown, tests have to be performed at different stress levels to allow for an evaluation of *n* according to eq. (9). This will dramatically increase the experimental effort.

For higher *n* values than the one in the present investigation, the time budget for the static tests can always be kept near the one demonstrated here, while the effort necessary to test specimens at a sufficient number of (slow) constant stress-rates can be even higher than in the presented case.

6. Summary and Conclusions

Static bend tests and constant stress-rate tests were used to determine the parameters for sub-critical crack growth, *n* and *B* of a commercial alumina ceramic. Several evaluation procedures were applied to the constant stress-rate data. All procedures lead to comparable values for *n* and *B*. There is a tendency that constant stress-rate tests provide more accurate results than the evaluation of the lifetime distribution. While *n* could be determined with reasonable scatter, the variety in *B* was much bigger.

An analysis of the experimental data revealed that the investigated material was especially easy to investigate. The value for the parameter *n* is rather low and the Weibull modulus of the inert strength distribution is high. Thus, a clear separation of the inert strength plateau from the SCCG influenced strength could be observed. A large range of stress-rates spanning five orders of

magnitude could be used for the evaluation. Constant stress-rate test were performed at such low stress-rates, that the same amount of crack growth as in the static bend tests was achieved.

Calculations of the crack growth behaviour were made to compare static and constant stress-rate tests. In static tests cracks start to grow immediately. The crack growth velocity increases gradually as the lifetime is approached. In constant stress-rate tests the crack starts to grow once a sufficient high stress is reached (in the investigated case after approximately 75% of the time to failure). Then the crack growth velocity increases dramatically until failure occurs.

The experimental effort for both types of tests was compared. Constant stress-rate tests can be done in approximately half the time needed for static tests, but still a minimum of two weeks will be necessary. These tests are also a prerequisite for successful ("short") static tests. Only if n is known, the stress level σ_{stat} can be chosen to achieve failure in reasonable timespans. Constant stress-rate tests as presented here are the method of choice if materials with low n and high m – values are to be tested. For other cases, (simple) evaluation methods have to be developed that consider all data – also those in the inert strength regime – and the scatter of data. To provide for an effective planning of such experiments it is desirable to get a more detailed insight into the mutual influence of m and n on constant stress-rate failure strength.

References

1 *Lawn, B. R.*: Fracture of Brittle Solids. Cambridge University Press, Cambridge (1993)

2 *Murakami, Y.*: The Stress Intensity Factor Handbook, Pergamon Press, New York (1986)

3 *Weibull, W.*: A Statistical Theory of the Strength of Materials, Generalstabens Litografiska Anstalts Förlag, Stockholm (1939)

4 *Wiederhorn, S. M.,* Subcritical Crack Growth in Ceramics. Fracture Mechanics of Ceramics, Bradt, R. C., Hasselman, D. P. H., Lange, F. F. (Eds.), Plenum Press, New York (1974), P. 613-646

5 *Michalske, T. A., and Freiman, S. W.*: A Molecular Mechanism for Stress Corrosion in Vitreous Silica. Journal of the American Ceramic Society, 66 (1983), P. 284-288

6 *Munz, D., and Fett, T.*: Ceramics, Springer, Berlin, Heidelberg (1999)

7 *Olagnon, C., Chevalier, J., and Pauchard, V.*: Global description of crack propagation in ceramics. Journal of the European Ceramic Society, 26 (2006), P. 3051-3059

8 *Richter, H., Kleer, G., Heider, W., and Röttenbacher, R.*: Comparative Study of the Strength Properties of Slip-cast and of Extruded Silicon-Infiltrated SiC. Materials Science and Engineering, 71 (1985), P. 203-208

9 *Nadler, P., and Schubert, E.*: Untersuchungen zur Sicherheit bei der Bestimmung des n-Wertes (Exponents des unterkritischen Rißwachstums). Fortschrittsberichte der DKG, 9 (1994)

10 *Pfingsten, T., and Glien, K.*: Statistical analysis of slow crack growth experiments. Journal of the European Ceramic Society, 26 (2006), P. 3061-3065

11 *Danzer, R.,* Ceramics: Mechanical Performance and Lifetime Prediction. The Encyclopedia of Advanced Materials, Bloor, D., Brook, R. J., et al. (Eds.), Pergamon, (1994), P. 385-398

12 *Wachtman, J. B.*: Mechanical Properties of Ceramics, Wiley-Interscience, New York, Chichester (1996)

13 *Danzer, R., Lube, T., Supancic, P., and Damani, R.*: Fracture of Ceramics. Advanced Engineering Materials, 10 (2008), P. 275-298

14 *EN 843-5*: Advanced Technical Ceramics - Mechanical properties of monolithic ceramics at room temperature: Part 5 - Statistical Evaluation, (2006)

15 *EN 843-3*: Advanced technical ceramics - Mechanical properties of monolithic ceramics at room temperature - Part 3: Determination of subcritical crack growth parameters from constant stressing rate flexural strength tests, (2005)

[16] *Baierl, R. G. A.*: Langsames Rißwachstum in Aluminiumoxid. Diplomarbeit, Institut für Struktur- und Funktionskeramik, Montanuniversität Leoben. (1999) 83

[17] *Davidge, R. W.*: Mechanical Behaviour of Ceramics. Cambridge University Press, Cambridge (1979)

[18] *Friatec*: Frialit-Degussit Oxidkeramik, Materialien, Anwendungen und Eigenschaften. http://www.friatec.de/content/friatec/de/Keramik/FRIALIT-DEGUSSIT-Oxidkeramik/downloads/de_Produkteigenschaften.pdf, (20.6.2011)

[19] *CEN EN 14425-5*: Fine Ceramics (Advanced Ceramics, Advanced Technical Ceramics) – Determination of Fracture Toughness of Monolithic Ceramics at Room Temperature by the Single-edge Vee-notched Beam (SEVNB) Method, (2005)

[20] *ASTM C 1368-06*: Standard Test Method for Determination of Slow Crack Growth Parameters of Advanced Ceramics by Constant Stress-Rate Flexural Testing at Ambient Temperature, (2008)

[21] *Peterlik, H.*: Comparison of Evaluation Procedures for the Subcritical Crack Growth Parameter *n*. Journal of the European Ceramic Society, 13 (1994), P. 509-519

[22] *Fett, T., and Gehrke, E.*: A Round Robin on Dynamic Bending Tests. Ceramic Forum International, 77 (2000), P. 7-11